

## Supplementary Information

Zhidong Ding<sup>1,#</sup>, Meng An<sup>1,2,#</sup>, Shenqiu Mo<sup>1,3</sup>, Xiaoxiang Yu<sup>1,3</sup>, Zelin Jin<sup>1,3</sup>, Yuxuan Liao<sup>4</sup>, Keivan Esfarjani<sup>5</sup>, Jing-Tao Lü<sup>6,\*</sup>, Junichiro Shiomi<sup>4,7,\*</sup>, Nuo Yang<sup>1,3,\*</sup>

<sup>1</sup> State Key Laboratory of Coal Combustion, Huazhong University of Science and Technology, Wuhan 430074, China

<sup>2</sup> College of Mechanical and Electrical Engineering, Shaanxi University of Science and Technology, Xi'an, 710021, China

<sup>3</sup> Nano Interface Center for Energy (NICE), School of Energy and Power Engineering, Huazhong University of Science and Technology, Wuhan 430074, China

<sup>4</sup> Department of Mechanical Engineering, The University of Tokyo, 7-3-1 Hongo, Bunkyo, Tokyo 113-8656, Japan

<sup>6</sup> Department of Mechanical and Aerospace Engineering, University of Virginia, Charlottesville 22904, United States

<sup>5</sup> School of Physical and Wuhan National High Magnetic Field Center, Huazhong University of Science and Technology, Wuhan 430074, China

<sup>7</sup> Center for Materials Research by Information Integration, National Institute for Materials Science, 1-2-1 Sengen, Tsukuba, Ibaraki 305-0047, Japan

# Z.D. and M.A. contributed equally to this work.

\* To whom correspondence should be addressed. E-mail: (J.-T.L.) [jtlu@hust.edu.cn](mailto:jtlu@hust.edu.cn),

(J.S.) [shiomi@photon.t.u-tokyo.ac.jp](mailto:shiomi@photon.t.u-tokyo.ac.jp), (N.Y.) [nuo@hust.edu.cn](mailto:nuo@hust.edu.cn)

## 1. Methods of band structure and thermoelectric (TE) coefficient calculations

The electronic structure is calculated through VASP<sup>1,2</sup>, which uses plane wave basis sets and PAW pseudopotentials. The Perdew-Burke-Ernzerhof (PBE) version of generalized gradient approximation (GGA) is used for the exchange-correlation potential<sup>3</sup>. The DFT-D2 method of Grimme is used to take into account van der Waals (vdW) interactions between different layers<sup>4</sup>. The convergence criteria for DFT self-consistent loops is set as  $10^{-4}$  eV. Atomic positions are fully relaxed until forces on all atoms are less than 0.05 eV/Å. In band structure and DOS calculations, a finer mesh of  $11 \times 11 \times 31$  is used.

With band structures obtained, the electrical conductivity  $\sigma$ , Seebeck coefficients  $s$  and the electronic thermal conductivity  $\kappa_e$  can be calculated from the Boltzmann transport equation (BTE) under the relaxation time approximation that is implemented in our modified version based on the BoltzTraP code<sup>5</sup>.

$$L^{(\alpha)} = e^2 \sum_n \int \frac{dk}{4\pi^3} \left( -\frac{\partial f(\varepsilon_{nk})}{\partial \varepsilon_{nk}} \right) \tau v_{nk} v_{nk} (\varepsilon_{nk} - \mu)^\alpha$$

$$\sigma = L^{(0)}$$

$$S = -(1/eT)\sigma^{-1}L^{(1)}$$

$$\kappa_e = 1/(e^2T)(L^{(2)} - L^{(1)}\sigma^{-1}L^{(1)})$$

where  $\varepsilon_{nk}$  is the energy eigenvalue of  $n$ th band at  $k$  point,  $f(\varepsilon_{nk})$  the Fermi-Dirac distribution function,  $\tau$  the momentum-dependent relaxation time,  $v_{nk}$  the group velocity,  $T$  the temperature and  $\mu$  the chemical potential, respectively.

The momentum-dependent relaxation time is calculated based on deformation potential approximation (DPA) proposed by Bardeen and Shockley <sup>6</sup>. The longitudinal acoustic phonon mode is considered in electron-phonon (e-ph) couplings along the direction of electricity flow. According to Shuai's work <sup>7</sup>,  $\tau$  can be expressed as follow,

$$\frac{1}{\tau_{e-ph}(k)} = \frac{\pi k_B E^2}{\hbar C} \sum_{k'} \delta[\varepsilon(k) - \varepsilon(k')] [1 - \cos\theta]$$

where  $E$  is the deformation potential constant for longitudinal acoustic phonons,  $C$  the elastic constant, and  $\theta$  the angle between  $k$  and  $k'$ , respectively.

In one-dimensional (1D) case, the relaxation time can be expressed as follow <sup>8</sup>,

$$\frac{1}{\tau_{e-ph}(k)} = \frac{k_B T E^2}{\hbar^2 C |v_k|}$$

Here,  $v_k$  is the group velocity, obtained through the derivative of energy to the wave vector,

$$v_k = \frac{1}{\hbar} \frac{\partial \varepsilon}{\partial k}$$

Define  $\varepsilon = (\hbar k)^2 / 2m^*$  and that  $m^*$  is the effective mass. The electronic mobility in 1D system can be obtained <sup>9</sup>,

$$\mu = \sqrt{\frac{2}{\pi}} \frac{C \hbar^2 e}{E^2 m^{*3/2} (k_B T)^{1/2}}$$

The elastic constant and the deformation potential constant of PCN are obtained from Figure S1, according to  $C = \partial^2 E_{total} / L_0 \partial \Delta L^2$  with  $\Delta L = \delta L / L_0$ , and  $E = \Delta E_{CB/VB} / \Delta L$ .  $E_{total}$  and  $\Delta E_{CB/VB}$  are the total energy and the energy difference of conduction (valence)

band minimum (maximum) respectively. The energy level of the deep core state is assume to be constant if the lattice deformation is small <sup>10,11</sup>. The lattice constant along  $z$  direction  $L$  is change, while  $L_0$  is the lattice constant at the equilibrium structure.  $C$  and  $E$  for the conduction band are 20.23 eV/Å and -3.95 eV, respectively. The doping effect is considered under rigid band approximation. Figure S2 shows the carrier concentration dependence of fermi energy. The two lines of fermi energy are nearly linear and display a similarly weak doping concentration with other materials obtaining 1D charge transport properties. The figure S3 shows the violation of the Wiedemann-Franz law.

## 2. Transfer integrals and the reorganization energy

We use the electronic band model to describe the charge transport in polymeric carbon nitride (PCN). It is commonly accepted that the band model can be used if electron transfer integrals  $\varepsilon$  are larger than or comparable to the reorganization energy <sup>12</sup>. For the validation, electronic transfer integrals  $\varepsilon$  and reorganization energy  $\lambda$  are calculated.

### 2.1 Transfer integrals

Transfer integrals  $\varepsilon$  of PCN are used to describe the hopping energy that is obtained by fitting conduction bands according to the tight-binding model <sup>13</sup>. The model for 1D bands is expressed as follow,

$$\varepsilon(\vec{k}) = \varepsilon_0 + 2\varepsilon \cos(\vec{k} \cdot \vec{L}_0)$$

We calculated the band structure with parameters provided in **Part 1**. Figure S2 shows results of the fitting, to be  $\varepsilon = 0.224, 0.216$  eV for the two conduction bands. The two valence bands do not behave like a cosine function and are much flatter than the conduction band. Therefore, it is clear that  $\varepsilon$  for valence bands are much smaller.

## 2.2 Reorganization energy

The reorganization energy is usually expressed as the sum of inner and outer contributions<sup>14</sup>. We use diabatic potential surfaces of melem to evaluate the inner part of reorganization energy. This value is assumed an upper limit of reorganization energy for PCN, because polymer chains and stacking motif impose more restrictions on geometrical optimization. As in most instances, the outer part is expected to have the same order of magnitude as the inner part<sup>14</sup>, the inner and outer parts are regarded as equal in our calculations.

We used Gaussian 09 to calculate the inner part of the reorganization energy<sup>15</sup>. The most stable structure of the neutral and cation state was determined by the structural optimization using B3LYP/6-31G(d, p). Then the total energies of the neutral state in the neutral structure ( $E$ ), the cation state in the cation structure ( $E_+$ ), the cation state in the neutral structure ( $E_+^*$ ), and the neutral state in the cation structure ( $E^*$ ) were calculated using B3LYP/6-31++G(d, p). The reorganization energy was obtained from

$$\lambda_{\text{inner}} = (E_+^* - E_+) + (E^* - E)$$

The inner part of reorganization we obtained is 0.148 eV for the melem monomer. The

total reorganization energy of PCN is 0.296 eV that is close to transfer integrals of its conduction bands.

### 3. MD simulation details

The lattice thermal conductivity of polymeric carbon nitrides (PCN) is calculated by equilibrium molecular dynamics (EMD) based on the Green-Kubo formula <sup>16</sup>,

$$\kappa = \frac{1}{3k_B T^2 V} = \int_0^\infty \langle \vec{J}(\tau) \cdot \vec{J}(0) \rangle d\tau \quad (1)$$

where  $\kappa$ ,  $k_B$ ,  $V$  and  $T$  are the thermal conductivity, the Boltzmann constant, and the volume of simulation cell, respectively.  $\vec{J}(\tau) \cdot \vec{J}(0)$  is the heat current autocorrelation function (HCACF). The angular bracket denotes ensemble average. The heat current is given by

$$\vec{J}(\tau) = \sum_i \vec{v}_i \varepsilon_i + \frac{1}{2} \sum_{i,j} \vec{r}_{ij} (\vec{F}_{ij} \cdot \vec{v}_i) \quad (2)$$

where  $\vec{v}_i$  and  $\varepsilon_i$  are the velocity vector and energy (kinetic and potential) of particle  $i$ , respectively.  $\vec{r}_{ij}$  and  $\vec{F}_{ij}$  are the interparticle separation vector and force vector between particles  $i$  and  $j$ , respectively. In MD simulation, the temperature  $T_{MD}$  is calculated from the kinetic energy of atoms according to the Boltzmann distribution:

$$\langle E \rangle = \sum_{i=1}^N \frac{1}{2} m v_i^2 = \frac{1}{2} N k_B T_{MD} \quad (2)$$

All the simulations are carried out utilizing the LAMMPS software package <sup>17</sup>. The repeating units of PCN are first constructed and put in an orthogonal unit cell with periodic boundary conditions in all directions. The expression of force field states <sup>8,18</sup>:

$$E_{\text{total}} = \sum_{\text{bonds}} K_r (r - r_{eq})^2 + \sum_{\text{angles}} K_\theta (r - r_\theta)^2 + \sum_{VDW} \varepsilon_{ij} \left[ \left( \frac{\sigma}{r_{ij}} \right)^{12} - \right.$$

$$2\left(\frac{\sigma_{ij}}{r_{ij}}\right)^6 + \sum_{Coul} \frac{Cq_i q_j}{\epsilon r_{ij}} \quad (3)$$

The parameters of bond, angle, VDW are taken from Ref. <sup>18</sup>, and listed in Table S1. The force-field has successfully predicted accurate thermodynamic properties of interests for our system of interest <sup>8</sup>.

The velocity Verlet algorithm is employed to integrate equation of motion, and the time step is set as 0.1 fs. At the beginning of thermal conductivity simulations, the system runs in the NVT ensemble for 500 ps. Then, the simulations run in the NPT ensemble for another 500 ps to relax the structure. After relaxation, the simulation is switched to run in the NVE ensemble and the HCACF is recorded for 1ns. Finally, the thermal conductivity is obtained by the integral of the HCACF (Eq.1).

#### 4. MD results and discussions

In EMD simulations, the cross-plane thermal conductivity of PCN shows a weak size dependence, which is related to the phonon wavelength <sup>19,20</sup>. Therefore, we examined the dependence of thermal conductivity on system size. It is noted that in Fig. S6 the thermal conductivity is converged when the simulation cell is 6×6×10 MD unit cells (100.35 Å × 76.11 Å × 7.28 Å) and the temperature is 250K. Therefore, the simulation cell size is taken in all the simulations.

Figure S8 shows that the thermal conductivity as a function of temperature. It is noted that thermal conductivity of PCN fluctuates in the range of 0.3~0.6W/m-K, which fall into the common range of 0.1~1.0 W/m-K for organic molecular crystals <sup>8</sup>. The low thermal conductivity originates from the weak intermolecular bonding of vdW nature,

compared with the strong intramolecular valence bonding. Besides, the thermal conductivity firstly increases, and then falls with the increasing temperature. The reason is that the more phonons are excited to contribute thermal transport as the temperature increases. Meanwhile, the phonon-phonon scattering would significantly increase in high temperature. Thus the thermal conductivity would decrease.

To accurately predict the lattice thermal conductivity of A-A stacked PCN along z direction, we consider vdW interaction and electrostatic forces to describe the overlap of  $p_z$  orbitals. The Normalized heat current autocorrelation function (HCACF) and lattice thermal conductivity along z direction at 300 K are shown in Fig. S9. In addition, we also calculate the thermal conductivity at different temperatures, shown in Fig. S10. By contrast, we observed that the thermal conductivity of PCN at 300 K is enhanced by 28.57 % when considering the electrostatic force to describe the overlap of  $p_z$  orbitals. Therefore, compared with the weak vdW interactions between interlayers, the overlap of  $p_z$  orbitals in PCN does noticeably enhance the thermal transport.

## References

- 1 G. Kresse and J. Furthmüller, *Phys. Rev. B*, 1996, **54**, 11169.
- 2 G. Kresse and D. Joubert, *Phys. Rev. B*, 1999, **59**, 1758.
- 3 J. P. Perdew, K. Burke and M. Ernzerhof, *Phys. Rev. Lett.*, 1996, **77**, 3865.
- 4 S. Grimme, *J. Comput. Chem.*, 2004, **25**, 1463–1473.
- 5 G. K. H. Madsen and D. J. Singh, *Comput. Phys. Commun.*, 2006, **175**, 67–71.
- 6 J. Bardeen and W. Shockley, *Phys. Rev.*, 1950, **80**, 72–80.
- 7 Z. Shuai, L. Wang and C. Song, *Theory of Charge Transport in Carbon Electronic Materials, SpringerBriefs in Molecular Science, Springer, Berlin, Heidelberg, Germany*, 2012, pp. 68–71.
- 8 X.-Y. Mi, X. Yu, K.-L. Yao, X. Huang, N. Yang and J.-T. Lü, *Nano Lett.*, 2015, **15**, 5229–5234.
- 9 F. B. Beleznav, F. Bogár and J. Ladik, *J. Chem. Phys.*, 2003, **119**, 5690–5695.
- 10 J. Xi, M. Long, L. Tang, D. Wang and Z. Shuai, *Nanoscale*, 2014, **4**, 4348–4369.
- 11 S.-H. Wei and A. Zunger, *Phys. Rev. B*, 1999, **60**, 5404.
- 12 V. Coropceanu, J. Cornil, D. A. Da, S. Filho, Y. Olivier, R. Silbey and J.-L. Brédas, *Chem. Rev.*, 2007, **107**, 926–952.
- 13 K. Hannewald, V. Stojanovic', J. M. T. MSchellekens, P. A. Bobbert, G. Kresse and J. Hafner, *Phys. Rev. B*, 2004, **69**, 075211.
- 14 J.-L. Brédas, D. Beljonne, V. Coropceanu and J. Cornil, *Chem. Rev.*, 2004, **104**, 4971–5004.
- 15 Frisch, M. et al. Gaussian 09, Revision A.02, Gaussian. Inc., Wallingford, CT

- 2009, **200**.
- 16 M. Kaviany, *Heat Transfer Physics*, Cambridge University Press, 2014, pp. 156–159..
  - 17 S. Plimpton, *J. Comput. Phys.*, 1995, **117**, 1–19.
  - 18 W. D. Cornell, P. Cieplak, I. Christopher, I. Bayly, I. R. Gould, K. M. Merz, D. M. Ferguson, D. C. Spellmeyer, T. Fox, J. W. Caldwell and P. A. Kollman, *J. Am. Chem. Soc.*, 1995, **117**, 5179–5197.
  - 19 J. Chen, G. Zhang and B. Li, *Phys. Lett. A*, 2010, **374**, 2392–2396.
  - 20 P. K. Schelling, S. R. Phillpot and P. Keblinski, *Phys. Rev. B*, 2002, **65**, 144306.

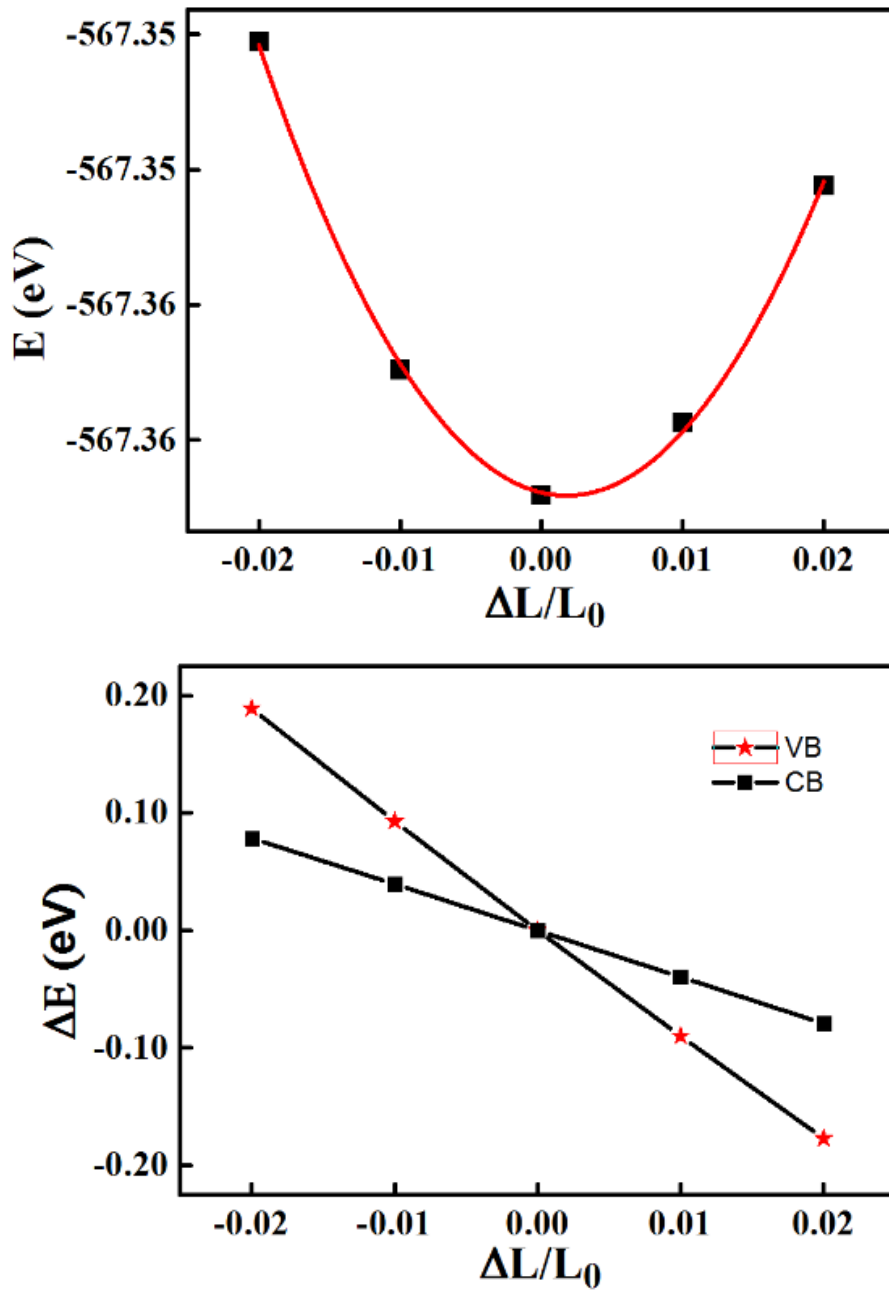


**Figure S1.** Upper: The total energy of a PCN unit cell as a function of the lattice dilatation along the  $c$  direction. Lower: The conduction and the valence band edge shifts as functions of the lattice dilatation.

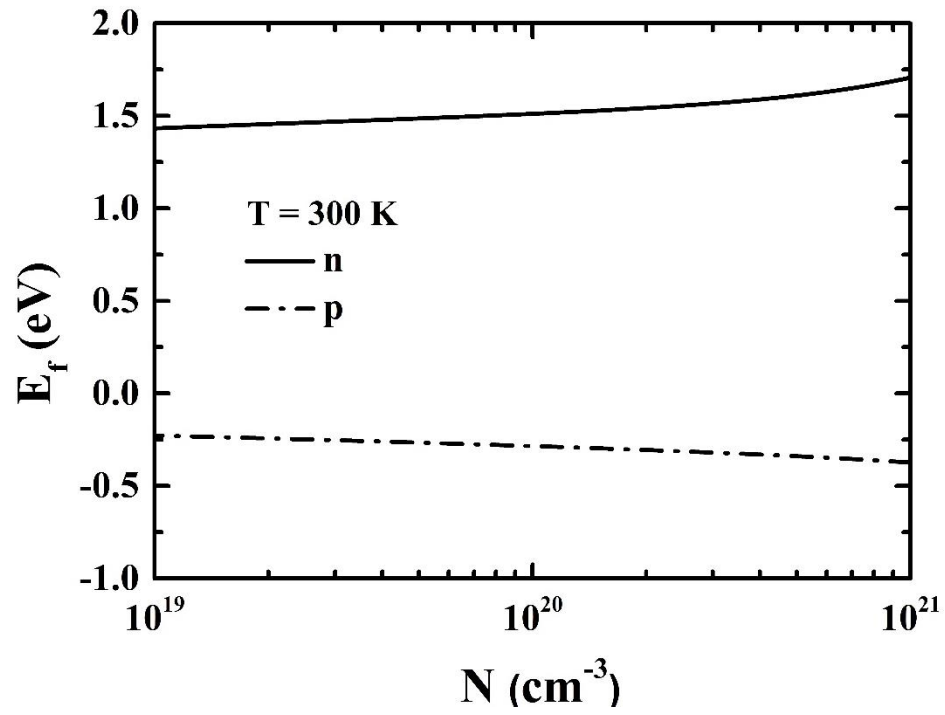


**Figure S2.** The carrier concentration dependence of Fermi energy at the room temperature.”

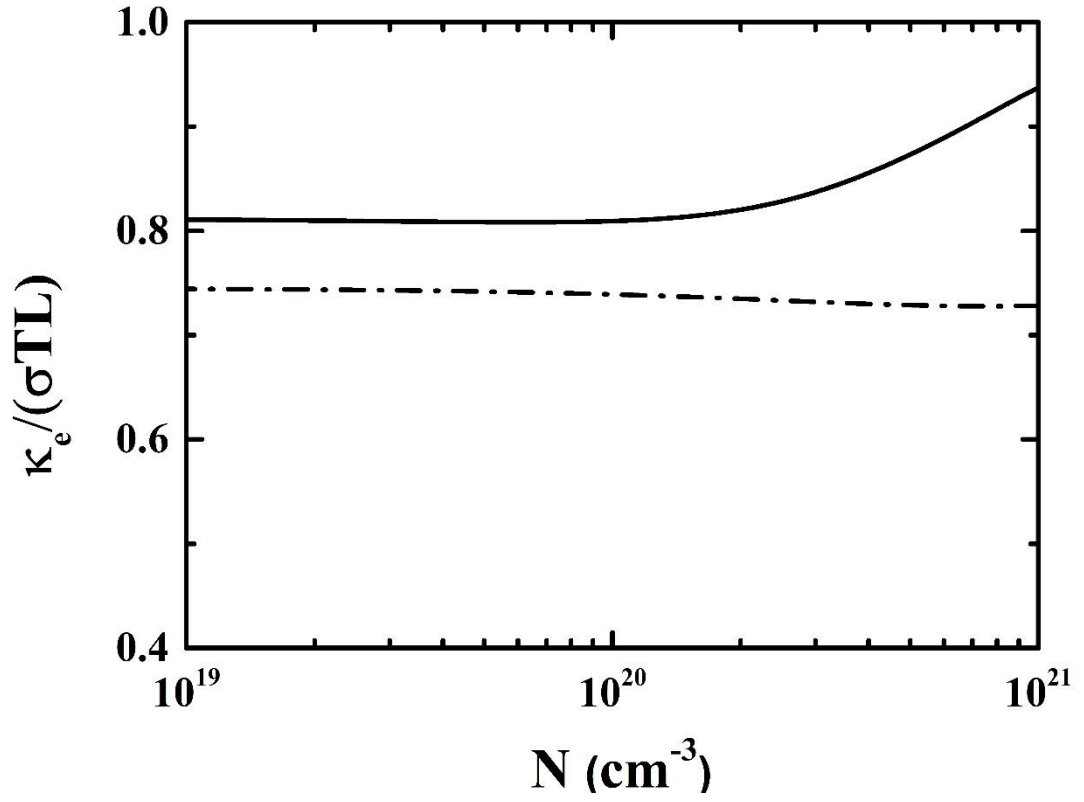
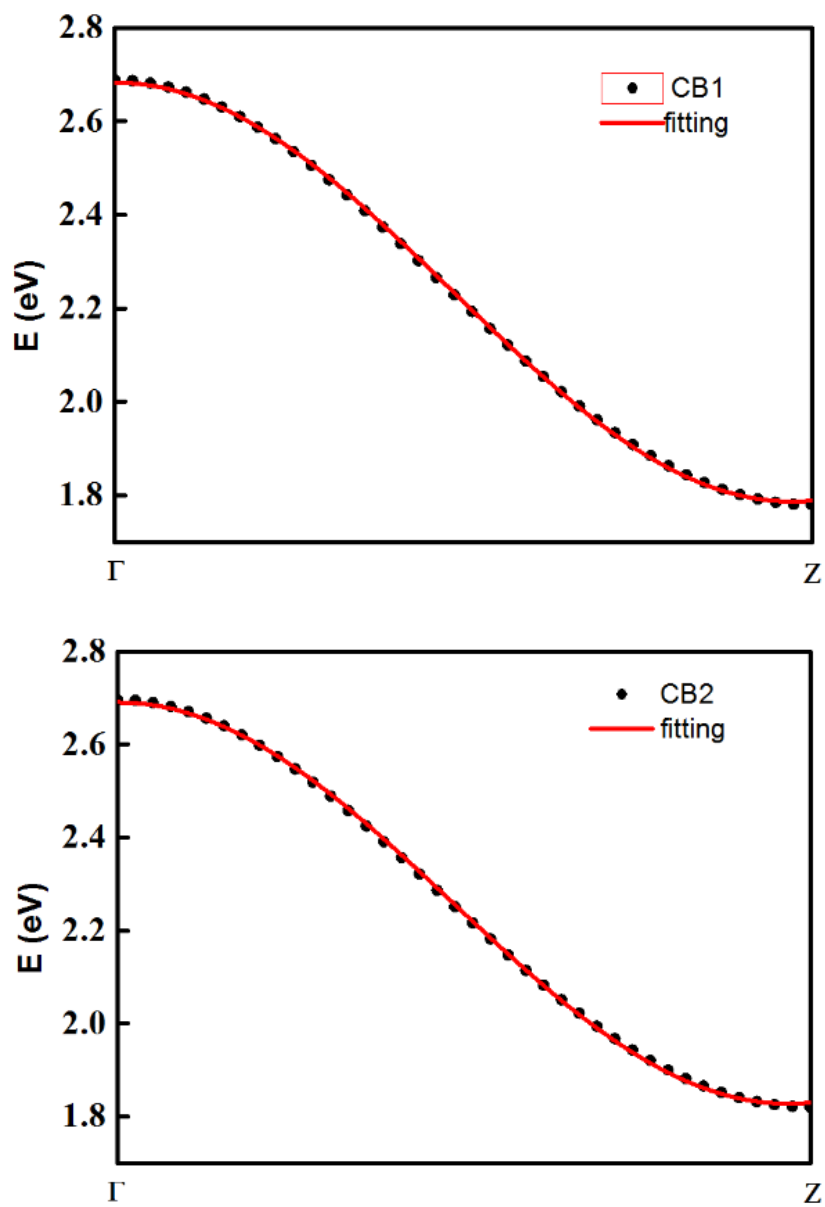
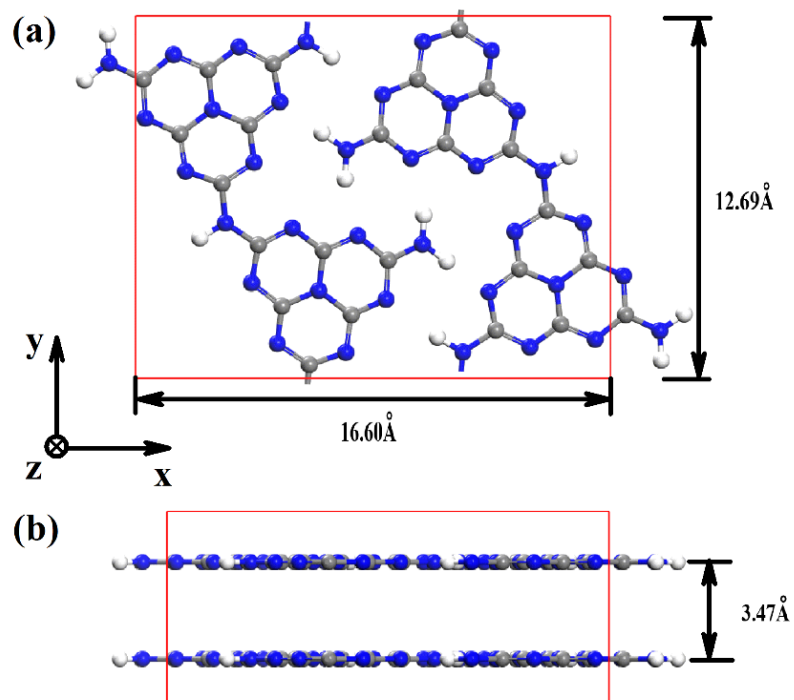


Figure S3, The  $\kappa_e/(\sigma TL)$  as a function of doping concentration.  $L$  is the Lorenz number,  $L = \pi^2 k_B^2 / (3e^2)$ , where  $k_B$  is the Boltzmann constant and  $e$  is the elementary charge.



**Figure S4.** The conduction band fitting from  $\Gamma$  to Z with the tight-binding model.



**Figure S5.** The structure of polymeric carbon nitrides. (a) The top view, a hexagonal simulation unit cell, and its length along the  $x$  ( $y$ ) direction is 16.60 Å (12.69 Å). (b) The side views. The interlayer distance is 3.47 Å. The blue atoms are Nitride, the black atoms are carbon and the white atoms are hydrogen.

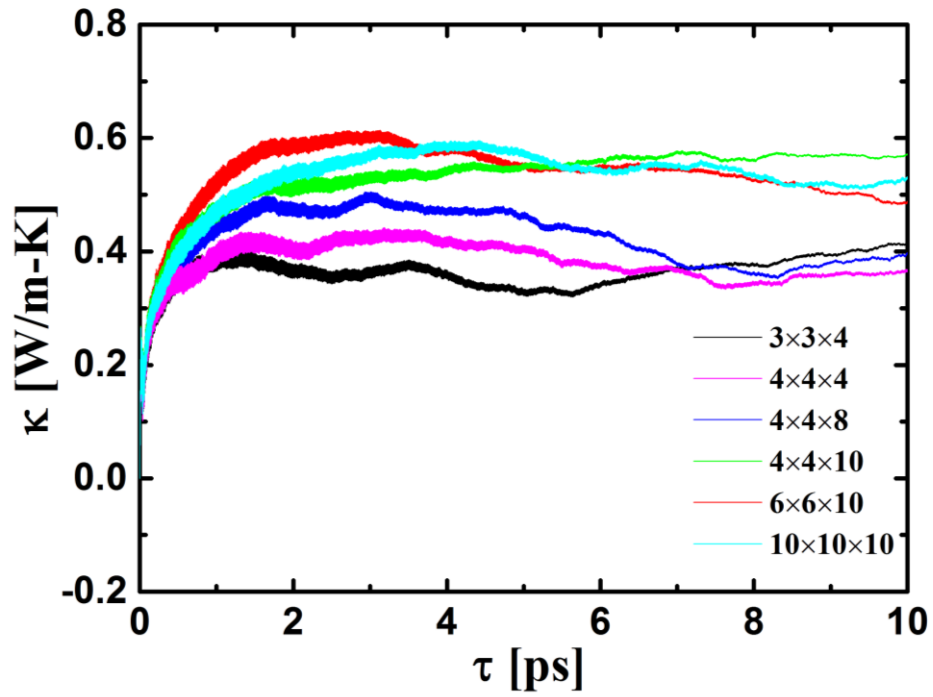


**Figure S6.** The lattice thermal conductivity along the  $z$  direction for simulation cell with different sizes. The simulation unit cell of  $1 \times 1 \times 1$  is  $16.60 \text{ \AA} \times 12.69 \text{ \AA} \times 3.46 \text{ nm}$ . The temperature of simulation is 250 K.

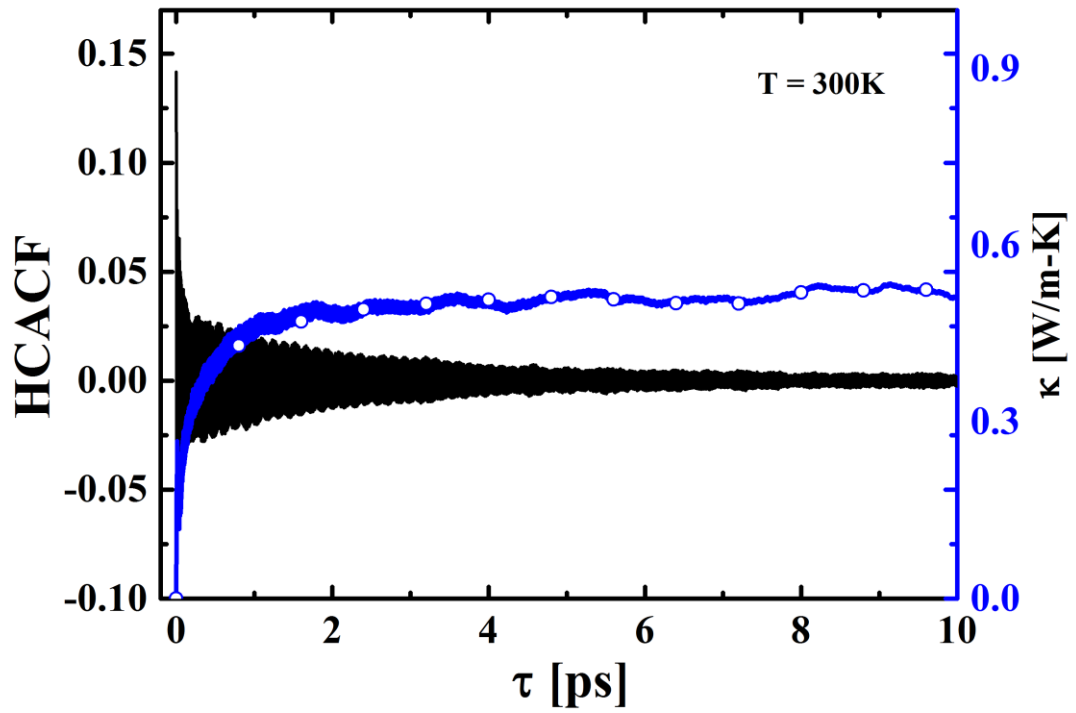


**Figure S7.** The heat current autocorrelation function (HCACF) along the  $z$  direction (black line). The right (blue line) axis corresponds to the lattice thermal conductivity from the integral of HCACF. The simulation supercell of  $6 \times 6 \times 10$  is  $100.35 \text{ \AA} \times 76.11 \text{ \AA} \times 7.28 \text{ \AA}$ .

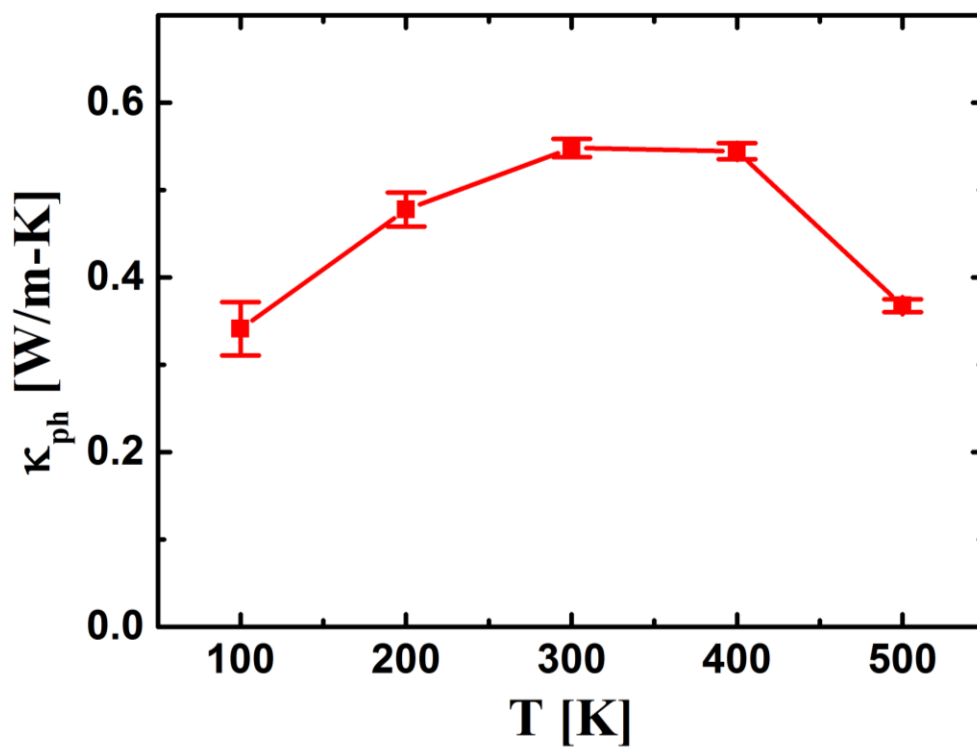


**Figure S8.** The lattice thermal conductivity of polymeric nitrides carbon as a function of temperature from the molecular dynamics simulations without considering the thermal contribution from electrostatic force to describe the overlap of  $p_z$  orbitals.

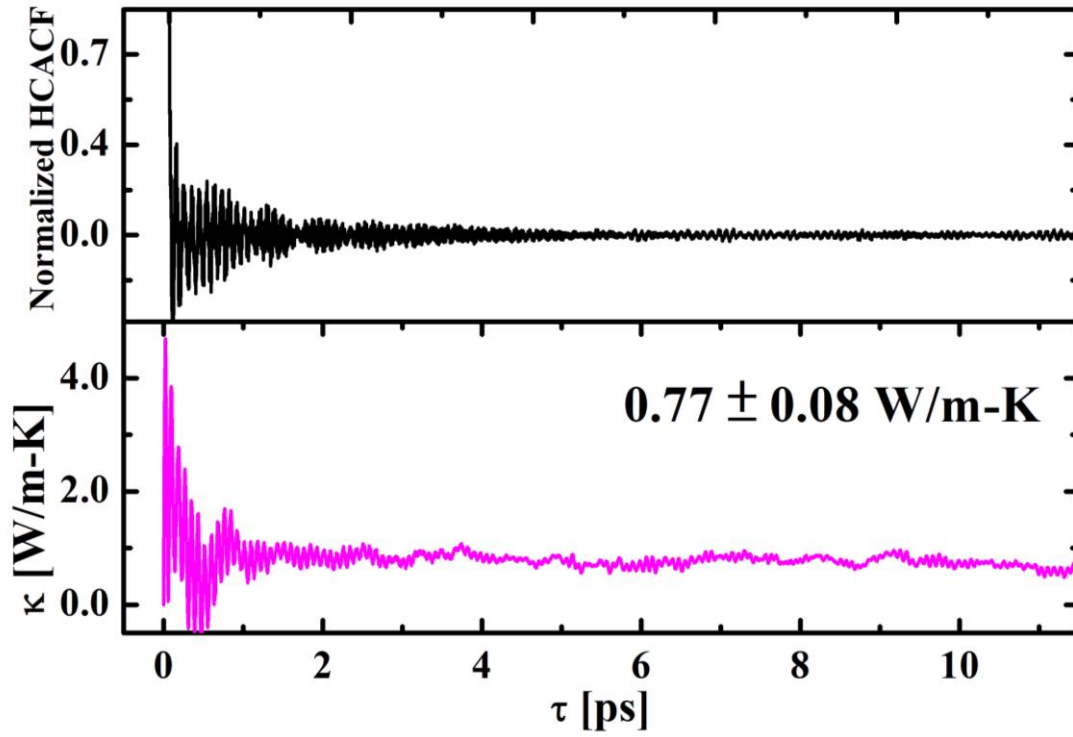


**Figure S9.** (a) Normalized heat current autocorrelation function (HCACF) along the  $z$  direction when we consider the electrostatic force to describe the overlap of  $p_z$  orbitals. (b) The lattice thermal conductivity along the  $z$  direction from the intergral of HCACF. The temperature is at 300 K.

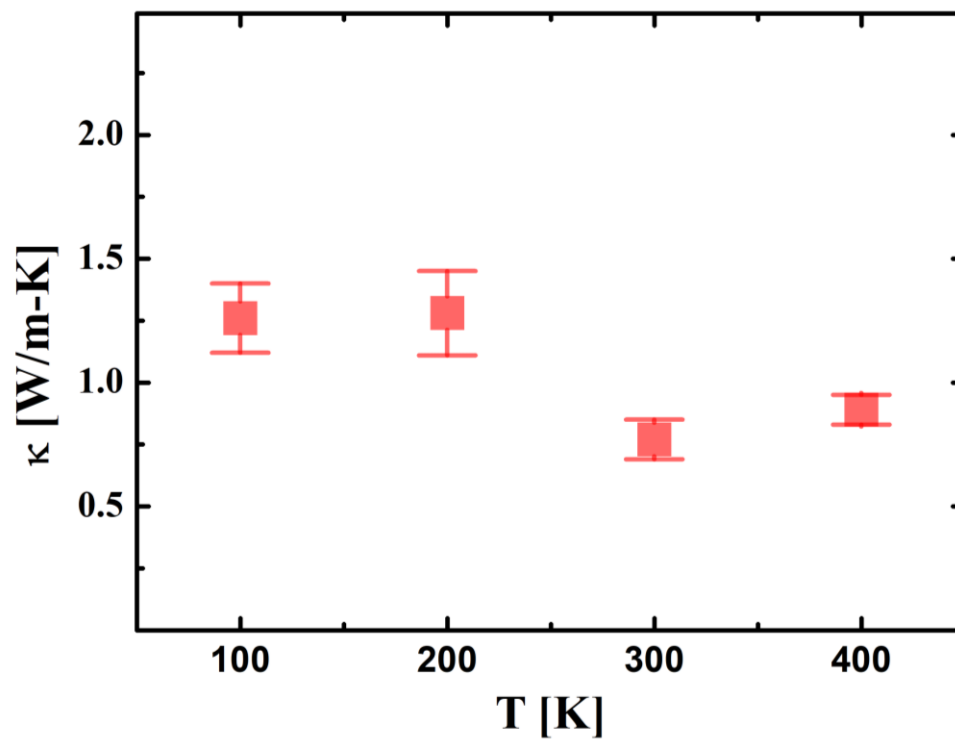


**Figure S10.** The lattice thermal conductivity of polymeric nitrides carbon as a function of temperature from the molecular dynamics simulations. We consider thermal conductivity contribution of the electrostatic force to describe the overlap of  $p_z$  orbitals.

**Table S1.** The parameters of bond, angle, VDW in potential functions. The  $\delta$  and  $\epsilon$  used in Eq. (1) for an interaction of atom I and atom j is  $\delta_{ij} = \delta_i + \delta_j$  and  $\epsilon_{ij} = \sqrt{\epsilon_i \epsilon_j}$ , respectively.

Bond Parameters		
bond	$K_r$ (kcal/(mol·Å <sup>2</sup> ))	$r_{eq}$ (Å)
CA-NA	227.0	1.1810
CA-NC	483.0	1.339
NC-H	434.0	1.010
N2=H	434.0	1.010
CA-N2	481.0	1.340
Angle Parameters		
angle	$K_\theta$ (kcal/(mol·radian <sup>2</sup> ))	$\theta_{eq}$ (degrees)
NA-CA-NA	70.0	120.00
NA-CA-NC	70.0	123.30
CA-NA-CA	70.0	112.00
CA-NC-CA	30.0	125.00
CA-NC-H	35.0	118.00
H-N2-H	35.0	120.00
CA-N2-H	35.0	120.00
NA-CA-N2	70.0	116.00
Van der Waals Parameters		

---

atom type	$\epsilon$ (kcal/(mol))	$\sigma$ (Å)
N	0.1700	1.8240
C	0.0860	1.9080
H	0.0157	0.6000

---